

## **Mesoscale convective vortices observed during BAMEX, Part I: Kinematic and thermodynamic structure**

Christopher A. Davis and Stanley B. Trier

National Center for Atmospheric Research<sup>1</sup>  
Boulder, Colorado

### **1. Background**

Midtropospheric mesoscale convective vortices (MCVs) of 50-300 km radial extent are a commonly observed structural component of many large mesoscale convective systems (MCSs). Their primary importance is as the dynamically balanced remnant of deep convection, which may persist as a coherent structure for many hours (or even days) beyond the decay of the initial convection within which the vortex forms. The MCVs appear intimately related to new convection downstream and appear to be the catalyst for some serial MCSs, i.e., MCSs on successive nights along a coherent propagation axis.

For a review of the science issues related to MCVs, the reader is referred to and Davis et al. (2004). The primary science objectives pertaining to MCVs are outlined in Davis et al. (2004). Briefly, these are:

- Observe and diagnose mechanism(s) of MCV formation
- Document the structures of mature MCVs, emphasizing vertical penetration, vortex tilt, radial vorticity profiles and first-order asymmetries.
- Diagnose vertical motion and vertical displacement induced by MCVs.
- Determine the cause of secondary convection near MCVs.
- Determine the effect of secondary convection on MCVs

### **2. Data and Analysis**

As summarized in Davis et al. (2004), BAMEX utilized two P-3 Orion aircraft, one from the Naval Research Laboratory (NRL) and the other from the National Oceanic and Atmospheric Administration (NOAA), and a Lear jet equipped with dropsondes. In addition, a ground based observing system (GBOS) consisting of three mobile GPS-Loran Atmospheric Sounding Systems (MGLASS) and the Mobile Integrated Profiling System (MIPS) from the University of Alabama, Huntsville, were used.

For MCV missions without appreciable precipitation near the vortex, the main deployment was the GBOS and the Lear jet with dropsondes. The Lear jet executed flight legs 200-300 km long across the vortex circulation. GBOS was deployed in a triangle on the downshear side so that the soundings from the triangles could be used to compute a time series of vertical motion. The number of soundings obtained during MCV missions ranged from about 18 to 31, spanning a 3-6 h period. The objective of the soundings was to sample both the vortex and its environment.

To enhance the dropsonde data in the analysis, we included profiler observations from times during the drop periods. Soundings and profilers were time-space corrected relative to approximately the central time of each

flight assuming an average translation speed of the MCV. This was estimated using radar animations to track the center.

To compute quantities such as divergence, vertical motion and relative vorticity, Bellamy (1949) triangles are defined. For each triangle (including any combination of time-space corrected profilers, dropsondes, and MGLASS), the divergence is simply the line integral of the normal wind component. The vorticity is the line integrall of the side-parallel component. Soundings were interpolated to a 10 hPa interval in the vertical from which omega was obtained as the vertical integral of divergence. Because we are interested in lower-tropospheric vertical velocity, we integrate only to 600 hPa and apply no integral constraint on divergence.

Having a collection of triangles, with parameters defined at the centroids, subjective and objective analysis was performed. Triangle sizes were confined between 1000 and 30000 km<sup>2</sup> with a maximum leg length of 200 km (300 km for IOP 15, Sec. 3c).

### 3. MCVs

In Table 1 we summarize each mature MCV case during BAMEX. All cases occurred within the southwestern part of the BAMEX domain. We estimated the maximum azimuthally averaged tangential wind ( $V_m$ ) and the radius at which it occurred ( $R_m$ ) for each case. The vortex of IOP 8 was the strongest and had the greatest circulation. The MCV of IOP 4 was the largest, but both IOP 4 and IOP 5 MCVs were clearly embedded within larger-scale troughs making assignment of a scale somewhat arbitrary.

IOP	1	4	5	8	15
date	5/24	6/2	6/5	6/11	6/29
Loc	OK AR	KS MO	TX	AR MO	KS
Fac	2,3,4	4	1,3,4	4	1,3,4
#snd	31	24	22	23	18
$V_m$	10- 12	10- 12	8-10	15	7
$R_m$	75	150+	100	150	100

Table 1. Summary of the five mature MCVs sampled during BAMEX. The estimated maximum azimuthally averaged tangential wind ( $V_m$ ) is in m/s; the radius of the maximum wind ( $R_m$ ) is in km.

#### *a. IOP 1*

As shown in Fig. 1, a bow echo preceded the MCV of IOP 1 (24-25 May). The bow echo formed over Nebraska during the evening of 24 May, moved south-southeastward and merged with another convective line forming in Kansas. The bow echo moved into Oklahoma around 1200 UTC before dissipating southeast of Oklahoma City around 1700 UTC. This system produced a long-lived MCV within which moderate and occasionally heavy stratiform rain with embedded deep convection was maintained throughout the day.

The MCV in IOP 1 was unique because it was sampled by all three aircraft. Only dropsondes from the WMI Lear jet will be discussed here. Thirty-one dropsondes were released during two sampling periods, the first from 1614 to 1734 UTC, and the second from 1950 to 2234 UTC. Nearly all drops were made from 180-190 hPa. There were problems recording winds on some soundings, but good thermodynamic data were obtained from all soundings.

The vortex motion, determined from animations of radar and satellite data, was about  $12 \text{ m s}^{-1}$  from  $280^\circ$ . This motion changed little during the day. Thus it was straightforward to merge the

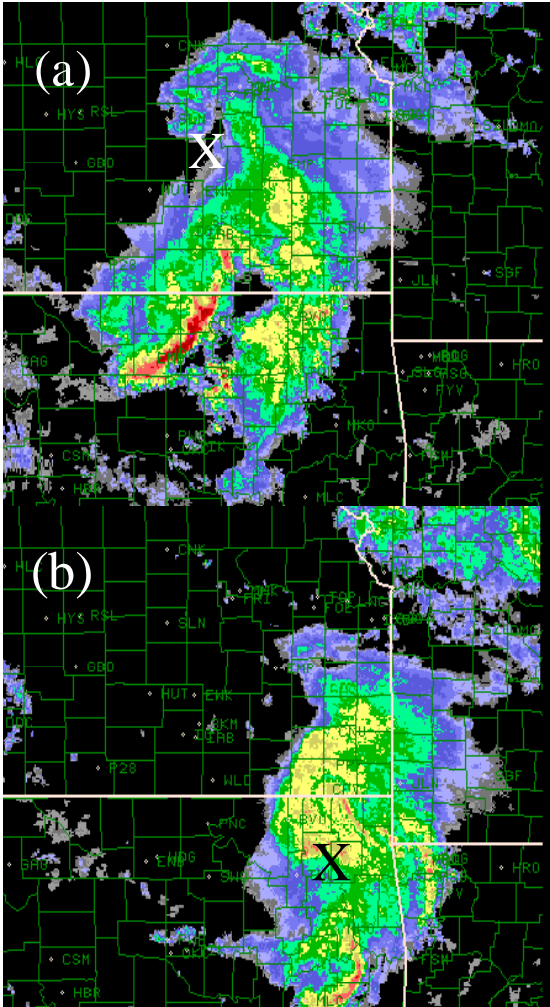


Figure 1. Composite radar images at (a) 1030 UTC 24 May, 2003 and (b) 1630 UTC 24 May. Yellow  $> 40 \text{ dBZ}$ ; red  $> 50 \text{ dBZ}$ . X's indicate (a) first MCV and (b) second MCV, the vortex discussed herein.

two time-space corrected datasets, at least at the pressure level near the maximum intensity. Those merged data at 600 hPa appear in Fig. 2, plotted in a vortex-relative spatial coordinate with the vortex motion subtracted. A composite dropsonde profile was used to convert height to pressure at profiler locations. Beneath this level, strong

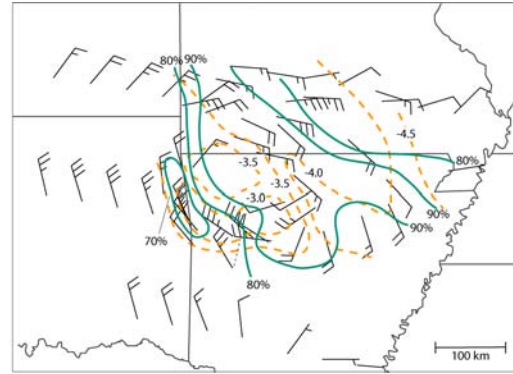


Figure 2. Analysis of temperature (orange, dashed) and relative humidity (green) and wind barbs at 600 hPa using soundings and profiles time-space corrected to 1930 UTC 24 May. Wind are system relative. Contour interval for temperature is  $0.5^\circ\text{C}$ ; for relative humidity it is 10%.

vertical shear (see Part 2) resulted in more structural transience, preventing a defensible merging of data from separate flights.

The plotted winds in Fig. 2

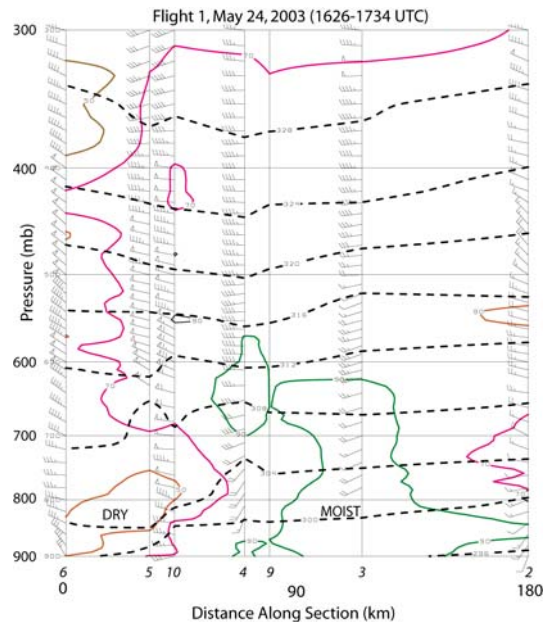


Figure 3. Vertical cross section oriented approximately east-west passing about 50 km south of the vortex center, constructed using dropsondes from flight 1. Green, magenta and brown contours indicate relative humidity of 90%, 70% and 50%, respectively. Potential temperature is contoured (dashed) with an interval of 4 K.

revealed a clear cyclone circulation centered over northwestern Arkansas with a radius of maximum wind near or slightly less than 100 km. The axis of the vortex appeared elongated from west-northwest to east-southeast, along the direction of both the vortex motion and the mean wind shear between 900 and 500 hPa, the latter being deduced from averaging the dropsondes. The maximum tangential wind was estimated to be 10-12 m s<sup>-1</sup>. There was little evidence of vortex-scale temperature perturbations in the core, suggesting that 600 hPa is close to the level of maximum tangential winds, assuming hydrostatic and gradient wind balance.

A cross section constructed from flight 1 (Fig. 3) shows that to the south

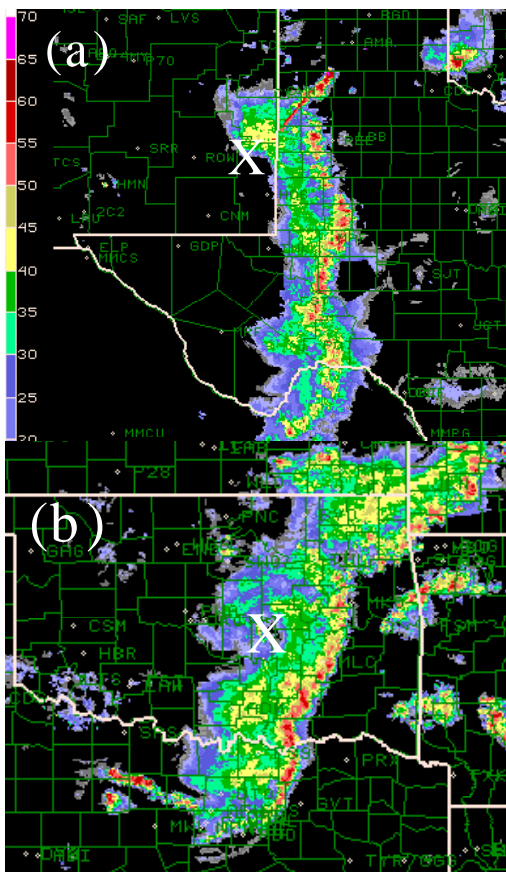


Figure 4. (a) Composite radar from 0400 UTC June 10 and (b) 0530 UTC June 11. MCV positions are indicated by X's.

of the vortex, the westerlies were slightly warmer and drier on this pressure level, but as one moved lower to the 900-800 hPa layer, the relative humidity decreased to below 50%. This lower-tropospheric dryness could be traced to subsidence behind the bow echo over northern Oklahoma earlier in the day.

### b. IOP 8

The strongest, largest and longest-lived of the five MCVs was sampled during IOP 8 on 11 June. The large-scale setting and life-cycle of the MCV and its attendant effects on lower-tropospheric frontal structure are summarized in Galarneau and Bosart (2004) elsewhere in this volume.

To provide a modest amount of context for this MCV, we show radar

#### 850 hPa Composite Analysis (1608-1902 UTC 11 June)

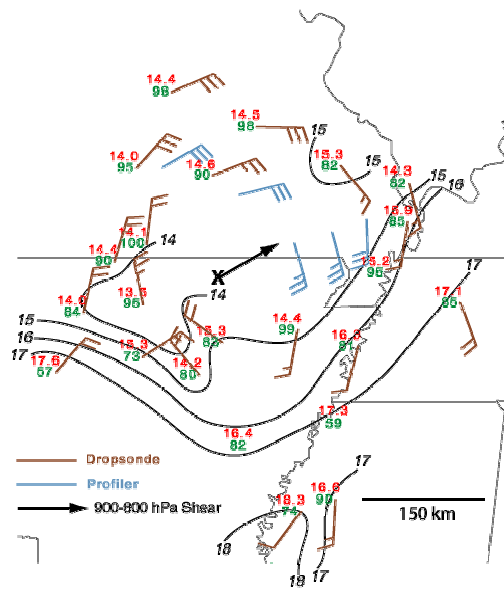


Figure 5. Station plots (red=temperature; green = relative humidity), wind barbs (brown = dropsonde, blue = wind profiler) and temperature contours (1oC interval), time-space corrected to 1730 UTC 11 June, 2003.

images in Fig. 4 from the early morning

hours of June 10 and June 11 that reveal the MCV grew out of two prior convective systems. There was clearly a vortex evident in the MCS that moved out of New Mexico on 9-10 June (Fig. 4a), based on profiler observations and radar reflectivity animations. The leading convective line moved southeastward through Texas while the MCV moved to the northeast. The background flow was such that the shear vector from ~0 to 3 km AGL was directed toward the southeast, but the lower-middle tropospheric wind was directed northeastward.

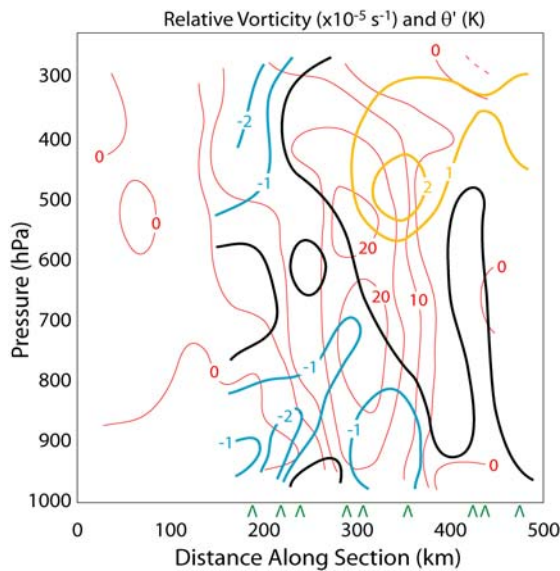


Figure 6. Vertical cross section (E-W through the vortex center) of vorticity (red, contour interval =  $5 \times 10^{-5} \text{ s}^{-1}$ ) and anomalous virtual potential temperature (gold  $> 0$ , cyan  $< 0$ , black = 0; 1 K interval). Green arrows indicate projection of sounding locations into cross section.

On the night of 10-11 June, an MCV was clearly evident within the stratiform region of the large MCS over Oklahoma. Whether this was an enhancement of the original center or a new center is not known. The vortex moved into northern Arkansas and southern Missouri during the daytime on 11 June.

The structure of the MCV is summarized in Fig. 5, in which we show an analysis of the temperature at 850 hPa, indicating the vortex core is cool relative to its surroundings at this level. The winds and temperature indicate pronounced lower-tropospheric temperature advection, warm advection to the southeast of the center and cold advection to the west. The wind at this level indicates a strong MCV. Maximum tangential winds near the level of maximum intensity (600-700 hPa) are almost uniformly  $15 \text{ m s}^{-1}$  around the vortex (system relative).

More information on the structure of the MCV is contained in a vertical cross section of vorticity and perturbation virtual potential temperature  $\theta'_v$  (Fig. 6). The vorticity is derived from triangles of time-space corrected dropsondes and wind profilers. The vorticity is gridded using a Cressman scheme with the values of vorticity valid at triangle centroids, and the influence of a triangle being inversely proportional to its area. The  $\theta'_v$  field is obtained by subtracting the mean vertical profile averaged over all soundings, and analyzing those soundings within 100 km of the plane of the cross section.

The vortex is deep, extending from the surface throughout the troposphere. Above 400 hPa, there is a tilt evident. We believe this is the signature of an upshear tropopause-based precursor cyclonic vorticity center analyzed by Galarneau and Bosart (2004). The MCV retains some of the canonical temperature structure with warm air above and cool air beneath the vortex. However, the dominant attributes of the temperature structure are asymmetries in the 'x' direction. In the lower and middle troposphere, warm air

dominates on the east side and cool air on the west side, consistent with vortex induced horizontal advection. Aloft, the cool air to the west of the vortex is consistent with cyclonic vorticity at the tropopause to the west of the MCV.

*c. IOP 15*

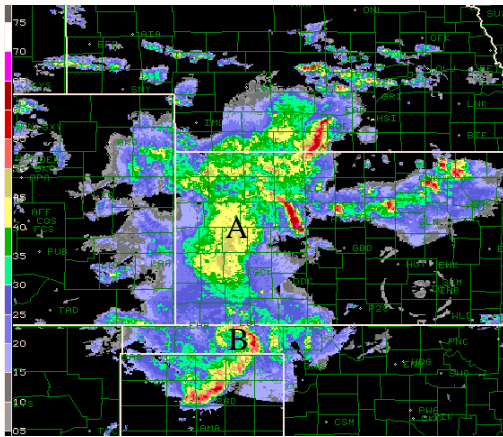


Figure 7. Composite reflectivity at 0500 UTC 29 June. 'A' denotes likely region in which MCV of IOP 15 formed. 'B' indicates another probable mesoscale vortex as evinced by radar image animation.

The MCV of IOP 15 originated among multiple convective systems over western Kansas on the night of 29 June, 2003 (Fig. 7). At present it is unclear whether the vortex arose from a single MCS or was a composite result of all the MCSs in the region. Regardless, a characteristic cyclonic swirl of radar echoes was evident beginning near 1100 UTC and indicated that an MCV was present in Central Kansas. Both MGLASS and the Lear jet were deployed to sample the MCV during the afternoon. The MCV is revealed by a plot at 750 hPa (Fig. 8), even though it attained its maximum intensity between 500 and 600 hPa (Fig. 9). An area of warm advection is evident on the southeastern flank of the vortex. This extends to the surface where it appears

that meridional winds associated with the vortex advected warm, moist air poleward, destabilizing the troposphere (see Part 2).

The vertical structure of the vortex is shown in Fig. 9. Unlike the MCV of IOP 8, there is almost no tilt of

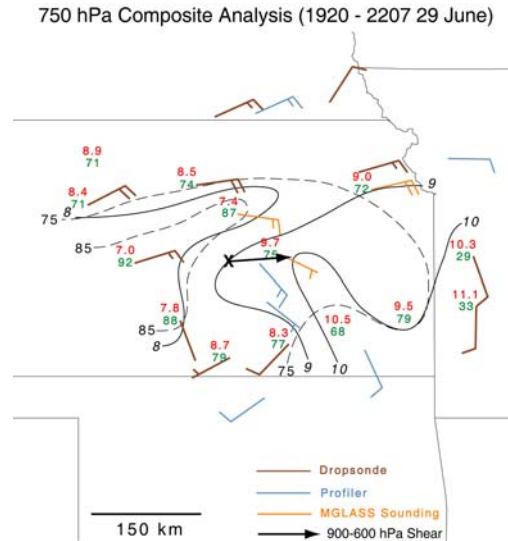


Figure 8. System-relative Winds at temperature at 750 hPa for IOP 15 (corrected to 2050 UTC). Colors are as in Fig. 6 except that gold wind barbs indicate an MGLASS sounding.

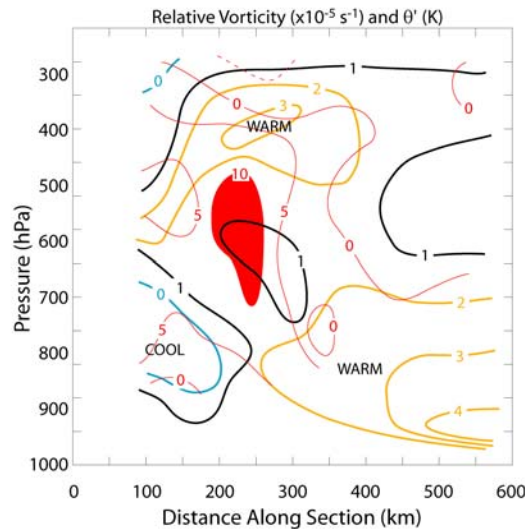


Figure 9. As in Fig. 7, but for IOP 15, valid 2050 UTC 29 June. Gold contours are used for  $\theta_v' > 1$  K. Dashed red line indicates relative vorticity  $< -5 \times 10^{-5} \text{ s}^{-1}$ .

the vortex in the upper troposphere. Instead an anticyclone is evident directly above the MCV, similar to the composite structure shown by Fritsch et al. (1994). This MCV penetrates to the surface, but there is a notable tilt over the lowest kilometer, also in contrast to IOP 8. This MCV maintains a maximum vorticity about half that of IOP 8.

The virtual potential temperature perturbation field (biased warm because the soundings were not evenly distributed around the vortex) shows warm air in the middle-upper troposphere between the cyclone and anticyclone. However, cool air is not evident beneath the MCV. Instead, a dipole pattern exists, consistent with vortex-induced temperature advection, with warm air to the east and cool air to the west. The pronounced warm air to the east of about  $x=400$  km is probably not vortex induced, but represents environmental inhomogeneity.

#### 4. Conclusions

In Part 1, we have examined the thermodynamic and kinematic structure of three of the five mature MCVs observed during BAMEX. Implications for convection retriggering will be explored in Part 2. In general, the MCVs collectively represent a sampling of different parts of a parameter space governed by intensity, and size. The MCV of IOP 8 was the strongest, had the greatest circulation and was the longest-lived. Davis et al. (2002) noted a relationship between vortex strength and longevity. However, it will be shown (Part 2) that the shear was also the weakest for IOP 1, suggesting that the MCV's longevity may have resulted from a lack of strain on the vortex. The MCVs in IOPs 4, 5 and 8 were all

clearly influenced by a larger-scale cyclonic vorticity feature, whereas the MCVs in IOPs 1 and 15 appeared to be relatively separated from larger-scale vorticity features (concerning structure only, not formation).

An important result shown by the detailed dropsonde and profiler data is that MCVs in IOPs 8 and 15 clearly penetrated to the surface. The MCV of IOP 8 induced warm frontogenesis in the boundary layer as well (not shown). Horizontal advection of temperature and moisture appeared strongly influenced by the MCV, leading to the appearance that the MCV was functioning as a small-scale baroclinic wave (or vortex), as noted by Jiang and Raymond (1995) based on idealized numerical simulations. This picture departs significantly from the classical picture of balanced MCVs wherein the primary temperature anomalies are above and below the core of the vortex. Whether this temperature structure was in a balanced state with the vortex will be assessed in future work.

#### References

- Bellamy, J. C., 1949: Objective calculations of divergence and vertical velocity and vorticity. *Bull Amer. Meteor. Soc.*, **30**, 45-49.
- Davis, C. A., D. A. Ahijevych, and S. B. Trier, 2001: Detection and Prediction of Warm Season, Midtropospheric Vortices by the Rapid Update Cycle. *Mon. Wea. Rev.*, **130**, 24-42.
- Davis, C., N. Atkins, D. Bartels, L. Bosart, M. Coniglio, G. Bryan, W. Cotton, D. Dowell, B. Jewett, R. Johns, D. Jorgensen, J. Knievel, K. Knupp, W.-C. Lee, G. McFarquhar, J. Moore, R. Przybylinski, R. Rauber, B. Smull, J. Trapp, S. Trier, R. Wakimoto, M. Weisman, and C. Ziegler, 2004: The Bow-Echo And MCV Experiment (BAMEX): Observations and Opportunities, *Bull. Amer. Meteor. Soc.*, August issue.

- Fritsch, J. M., J. D. Murphy, and J. S. Kain, 1994: Warm core vortex amplification over land. *J. Atmos. Sci.*, **51**, 1780--1807.
- Galarneau, T. J., Jr., and L. F. Bosart, 2004: The long-lived MCV of 11-13 June 2003 during BAMEX. *Preprints, 22<sup>nd</sup> AMS conference on Severe Local Storms*, Hyannis, MA. American Meteorological Society, paper 5.4
- Jiang, H., and D. J. Raymond. 1995: Simulation of a Mature Mesoscale Convective System Using a Nonlinear Balance Model. *J. Atmos. Sci.*, **52**, 161–175.